Comprehensive analysis on the performance of an IGCC plant with a PSA process integrated for CO_2 capture

Luca Riboldi[a,1], Olav Bolland[a]

[a]*Energy and Process Engineering Department, the Norwegian University of Science and Technology, NO-7491Trondheim, Norway*

Abstract

The main goal of this paper is to provide a comprehensive overview on the performance of an Integrated Gasification Combined Cycle (IGCC) implementing CO_2 capture through a Pressure Swing Adsorption (PSA) process. The methodology for integrating a PSA process into the IGCC plant is first defined and then a full-plant model is developed. A reference case is outlined both for the PSA-based plant and for an absorption-based plant. Physical absorption is considered the benchmark technology for the application investigated. The full-plant model allowed an assessment of the potentials of PSA in this framework. The plant performance obtained was evaluated mainly in terms of energy penalty and CO_2 separation efficiency. Several process configurations and operating conditions were tested. The results of these simulations demonstrated the influence of the PSA process on the overall performance and the possibility to shape it according to specific requirements. A sensitivity analysis on the adsorbent material was also carried out, aiming to establish the possible performance enhancements connected to advancements in the material. Improving the properties of the adsorbent demonstrated to have a strong impact not only on the CO_2 separation process but also on the performance of the entire plant. However, nor modifications in the process or in the material were able to fully close the gap with absorption. In this sense a synergetic approach for addressing further performance enhancements is outlined, based on the close collaboration between process engineering and material science.

Keywords: CO_2 capture, PSA, IGCC, process simulations

1. Introduction

The world is at a critical juncture in its efforts to contrast climate change. A comprehensive strategy is an impelling issue as further postponements would increase significantly the cost and the difficulty to meet the 2°C limit for the temperature increase. Greenhouse-gas emissions from the energy sector represent roughly two-thirds of all anthropogenic greenhouse-gas emissions. Effective action in the energy sector is, consequentially, essential to tackling the climate change problem [1]. Many scenarios published by independent institutions show that a long-term decarbonisation path cannot do without Carbon Capture and Storage (CCS). CCS enables a strong reduction of net CO_2 emissions from fossil-fuelled power plants and industrial processes, providing a protection strategy for power plants that cannot be thought to be completely dismantled in a realistic scenario of a carbon-constrained world [2]. The estimated cost of not including CCS in the toolbox would be prohibitive. An important milestone was recently achieved when the first commercial-scale CCS power plant came online in Canada (SaskPower Boundary Dam Unit 3). Globally, there are other 13 large-scale CCS projects in operation,

[1] Corresponding author. Tel.: +47 735 93559;
E-mail address: luca.riboldi@ntnu.no (L. Riboldi)

with a further nine under construction [3]. The outlook on the strategic role of CCS highlights the importance of investigating more and more efficient technologies for capturing CO_2 from various sources. Among other options, this paper focuses on Pressure Swing Adsorption (PSA) as a methodology for separating CO_2 from a gas mixture in the power sector. PSA is a cyclic process based on the ability of some solid adsorbents to selectively attract and fix CO_2 molecules on their surface. Before the adsorbent bed gets completely saturated, the feed is stopped and a regeneration process is carried out. When the regeneration of the adsorbent is performed by reducing the total pressure of the system, the process is termed PSA. PSA has been considered for its potential low energy requirements. Especially in pre-combustion applications, where the pressure is not reduced below atmospheric conditions, the main energy consumption is caused by the CO_2 compression. Thermal energy duty is generally avoided. Furthermore, a relatively low environmental impact has been predicted in the literature [4]. The technology can be adopted for several industrial applications, including CCS [5, 6], and an extensive literature can be found regarding processes [7] and materials adopted [8]. In a previous work we provided with a first assessment on the feasibility of large scale PSA process for removing and concentrating CO_2 in coal-fired power plants, both in a post- and pre-combustion scenario [9]. PSA showed to have the opportunity to become competitive with absorption, the most mature technology currently available, on an energy and CO_2 separation point of view. However, the large plant footprint estimated for the post-combustion case appeared to be a significant obstacle to further developments for that application. Pre-combustion case did not face such problem, so a detailed analysis of an IGCC plant integrating a PSA process is carried out in this paper. PSA demonstrated to be a promising option for removing CO_2 from the syngas of an IGCC plant if the separation process occurs at high temperature levels [10]. Also when combined with the shift process, a concept called Sorption Enhanced Water Gas Shift (SEWGS), PSA performs efficiently [11], albeit needs to address some challenges relative to the operability of the systems [12]. The same challenges apply to any system configuration involving a PSA process in pre-combustion applications. The current paper analyses the range of performances achievable by implementing a cold PSA separation (i.e., the syngas is cooled down after the Water Gas Shift section to proper temperature for the gas removal processes). In line with a previous work [9], the process arrangement adopted is to consider a single PSA train. A dual PSA system may allow obtaining higher separation performance. On the other hand, it would imply an increase of the footprint and consequently of the capital costs. The additional PSA train can become more attractive when pure H_2 has to be produced. An interesting example is the demonstration project located within the Valero refinery in Port Arthur (Texas) [13], where the syngas from two steam-methane reformers is processed in a dual PSA system to produce H_2 and capture CO_2. Within the framework considered in this work, a composite model has been developed which allows simulating the IGCC-PSA plant defined. Two main domains were considered for the performance investigation, namely the process configuration and the adsorption material. Modifications in the process layout and in the operating conditions were proposed and studied at a system level by means of the full-plant model developed. The impact of advancements in the adsorbent material was also studied. A sensitivity analysis on some targeted material properties was carried out and the effect evaluated on the separation process and on the overall plant. The outputs of all the process simulations were evaluated through a series of performance indicators defined to represent the energy and CO_2 capture efficiency of the plant. The basis for comparison was set to be an IGCC integrated with a physical absorption unit for CO_2 removal.

2. The IGCC plant integrating a PSA process

2.1. Plant model and layout

In order to model the IGCC-PSA plant two different simulation tools have been used. The gasification and gas treatment section, the power station, and the CO_2 compression unit have been modeled in Thermoflex (Thermoflow Inc.) [14]. PSA is a batchwise process, thus a dynamic model needed to be defined. A dynamic 1-dimensional model was developed in gPROMS (Process System Enterprise) [15]. It is constituted by a set of partial differential and algebraic equations (PDAEs), representing material, energy and momentum balances in the packed bed. A more detailed description of the model and of the solution of it can be found in [9]. The two models described were connected through an excel interface in order to exchange information. Even though the PSA process is inherently dynamic, it reaches something defined as Cyclic Steady State (CSS). CSS occurs when the conditions at the end of the cycle are exactly the same observed at the beginning. The occurrence of CSS and the utilization of several columns working in parallel assure the operating continuity of the system: the PSA can be connected to the rest of the plant which is working in a steady-state mode. The layout of the whole IGCC-PSA plant is represented in **Figure 1**. For a detailed description of the various units and of the integrating principles reference can be made to [9, 16]. The gasification takes place in an entrained flow dry-fed gasifier with convective gas cooler. Coal used is a Douglas Premium Bituminous Coal. The gasification pressure is set to 44.9 bar and the temperature to 1550°C. The syngas undergoes a shift process and acid gases are removed by a single-stage Selexol process. The PSA process separates CO_2 from the rest of the syngas which is fueling the power island. A combined cycle is producing a gross power output of about 460 MW. The gas turbine is a F class type. The bottom steam cycle features 3 pressure levels with reheat. The CO_2-rich stream is sent to the compression station, where it is further purified by means of a two-steps flash separation and it is delivered at 110 bar for transportation.

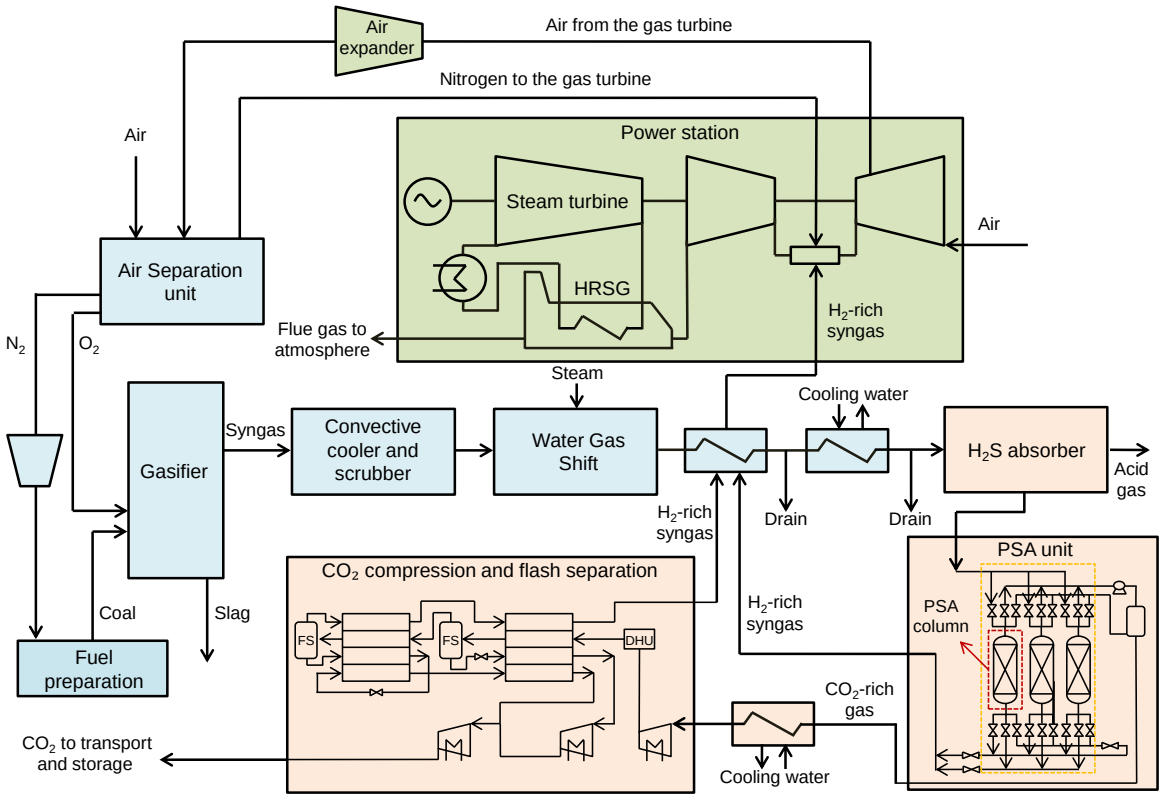

Figure 1. Flowsheet of the IGCC plant integrating a PSA unit for CO_2 capture.

2.2. *Base case process conditions and specifications*

In order to be able to carry out a thorough performance analysis on the defined IGCC plant with CO_2 capture, a base case needs to be defined. The choice of this base case is arbitrary and is necessary to understand the influence of different modifications introduced. The selection has been based on a previous work [9]. The instance selected demonstrated to return a good balance between separation and energy performances, and takes into consideration the operating constraints given by the integration of PSA into the IGCC plant. Most of the operating parameters are taken from EBTF [16], in order to set a defined framework for fair comparisons of the results. The pressure, the mass flow rate and the composition entering the PSA unit are dictated by the process upstream. The CO_2-rich gas stream leaving PSA needs to be compressed to 110 bar for transportation, with a CO_2 volumetric concentration above 95% [17]. The second product stream leaving PSA is rich in H_2. It has to be fed to the combustor of the gas turbine, thus it needs to fulfill specifications in terms of pressure (with a lower limit of 24.12 bar) and temperature (as high as 230 °C in accordance with the syngas pre-heating system). Within the mentioned constraints, the operating conditions of the PSA process and of the CO_2 compression process could be freely chosen. **Table 1** shows the values of the most significant ones. The PSA process relies on a 7-bed 12-step cycle and it was defined in order to fulfill the specifications of the two product streams in the most effective way. **Figure 2** shows the sequence of steps undergone by each column of the PSA unit and the scheduling of the cycle. More on the definition of the PSA cycle and on its optimization can be found in a previous work [9]. The adsorbent material selected is a commercial activated carbon [18].

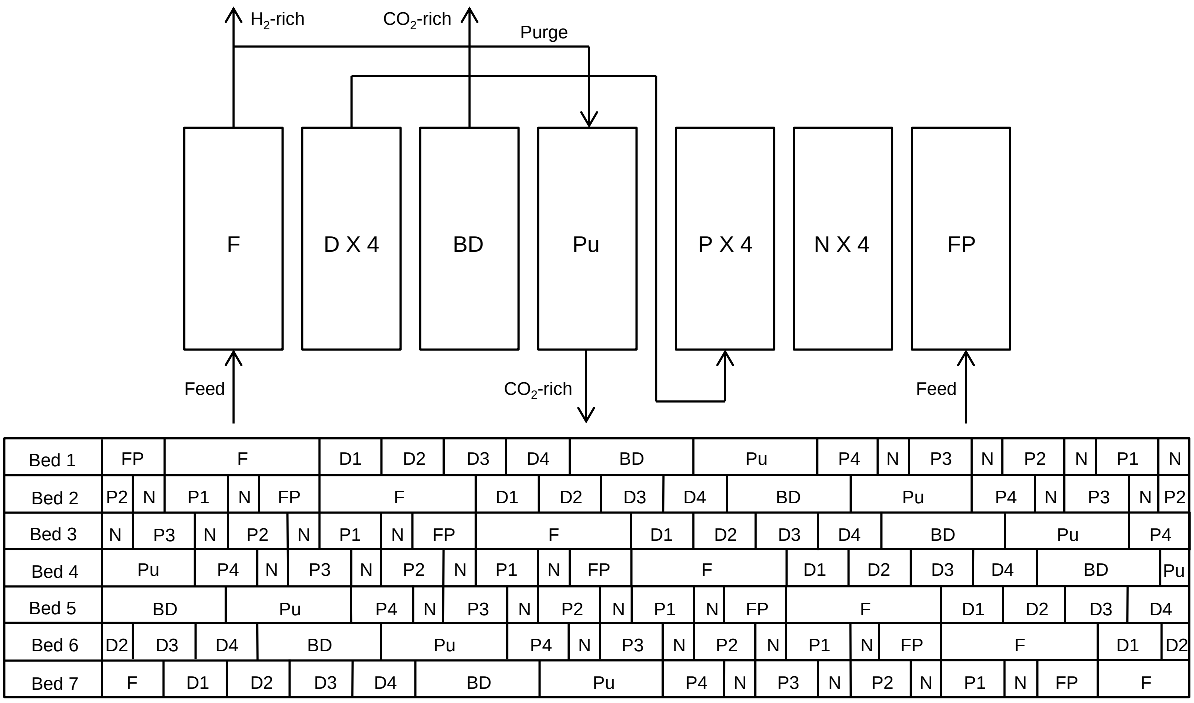

Figure 2. Scheduling of steps undergone by a column in the PSA cycle. The steps considered are: Feed Pressurization (FP), Feed (F), Pressure equalization - Depressurization (D), Blowdown (BD), Purge (Pu), Pressure equalization - Pressurization (P), Null (N).

Table 1.Operating parameters and characteristics of the base case selected

CO_2 compression and flash separation	
Flash pressure (bar)	30
Delivery pressure (bar)	110
T flash 1* (K)	243,2
T flash 2* (K)	218,7
PSA	
Adsorption pressure (bar)	38,8
Regeneration pressure (bar)	1
Syngas composition (% vol.) (CO_2 - H_2 - CO - N_2)	0,380 - 0,537 - 0,016 - 0,067
Syngas temperature (K)	338
Syngas flow rate (mol/s)	5331,7
P/F ratio	0,10
PSA cycle time (s)	630
t_{feed} (s)	90
$t_{pressure\ equalization}$ (s)	41
$t_{blowdown}$ (s)	80
t_{purge} (s)	59
t_{null} (s)	8
$t_{feed\ pressurization}$ (s)	41
PSA column characteristics	
Bed length (m)	10
Bed diameter (m)	6,6
Bed porosity	0,38
Solid density (kg/m^3)	1939

*T flash is the temperature of the gas stream entering the flash separators

The performance of the defined base case is shown in **Table 2**. The performance indicators utilized aims to give an assessment of the energy and CO_2 separation efficiency of the system. They include the net electric efficiency (η_{el}), the H_2 recovery (R_{H2}), the CO_2 recovery (R_{CO2}), the CO_2 purity (Y_{CO2}) and the CO_2 separation efficiency (η_{CO2}).These quantities are defined as following:

$$\eta_{el} = \frac{\text{Net electric output}}{\text{Thermal power input}_{LHV}} \tag{1}$$

$$R_{H_2} = \frac{\dot{m}\text{ of } H_2 \text{ entering the gas turbine as fuel}}{\dot{m}\ H_2 \text{ entering the } CO_2 \text{ separation unit}} \tag{2}$$

$$R_{CO_2} = \frac{\dot{m}\text{ of } CO_2 \text{ in the product stream}}{\dot{m}\text{ of } CO_2 \text{ formed}} \tag{3}$$

$$Y_{CO_2} = y_{CO_2} \text{ in the product stream} \tag{4}$$

$$\eta_{CO_2} = 1 - \frac{\eta_{net} \text{ for the reference plant without } CO_2 \text{ capture}}{\eta_{net} \text{ for the plant implementing } CO_2 \text{ capture}} \left(1 - R_{CO_2}\right) \tag{5}$$

When the recovery and the purity are referring only to the PSA process, thus not including the flash separation, the performance indicator is reported with the prefix PSA (e.g., PSA-R_{CO2}).
Considerations on the footprint of the separation unit are also present, taking into account the dimensions of the columns used for the different CO_2 separation technologies (the footprint values reported are simply the total square meters occupied by the separation columns).
Table 2 shows also results for an IGCC plant not implementing CO_2 capture and compression (simulated in Thermoflex) and for an IGCC plant integrating a two stage Selexol process, which is considered to be the most common commercial technology for removing CO_2 and H_2S [19]. The description of these systems can be easily found in the literature [16, 20]. Three cases for the absorption method are reported. A first one is the result of Thermoflex modeling and simulation. The utilization of the same modeling tool assures that identical assumptions for the IGCC plant in the PSA and absorption cases are applied. Nevertheless, Thermoflex assumes a constant value for the CO_2 purity in the absorption unit, equal to 100%. The value is overestimated as typical values range around 99%. This led to a consequent overestimation of the energy performance, since no H_2 is leaving with the CO_2-rich stream to be compressed. For this reason, two additional sets of results were taken from the literature, in order to get a more thorough overview of the state-of-the-art of absorption for CO_2 separation in this pre-combustion application.

Table 2. Overview of the performance of an IGCC plant with and without CO_2 capture.

	No Capture	**Absorption 1**	**Absorption 2 [16]**	**Absorption 3 [11]**	**PSA**
η_{net} [%]	47,3 %	37,1 %	36,7 %	36,0 %	36,2 %
R_{H2} [%]	-	100,0 %	99,3 %	99,7 %	99,6 %
Y_{CO2} [%]	-	100,0 %	98,2 %	99,0 %	98,9 %
R_{CO2} [%]	-	90,6 %	90,9 %	90,3 %	86,1 %
η_{CO2} [%]		88,1 %	88,3 %	87,2 %	81,8 %
Footprint (m^2)	-	8	-	-	239

3. Process configuration and operating conditions

In this section the performance of the IGCC-PSA plant is analyzed by investigating different process configurations and operating conditions. The results will be shown in terms of η_{net} and η_{CO2} for the overall plant. Although many of the modifications regard the PSA process, the output is studied at the system level. Previous studies investigated the optimum operating configuration for the separation unit alone [21]. However, the plant is highly integrated and modifications in the separation unit affect significantly the other units. The full-plant model developed allows to analyse these effects.
In the following sub-sections alternative process configurations or operating conditions are suggested. The resulting outputs are described and analysed. Most of the time, a set of results is graphically shown for each case studied. It refers to the system operating within the outlined conditions, but with different

Purge-to-Feed (P/F) mole flow rate ratio of the PSA process. An increase of P/F causes a decrease of PSA-Y_{CO2} and an increase of PSA-R_{CO2}. The effect on the whole system is a reduction of η_{net}. This indication can be utilized to understand in which direction P/F is changing in the figures proposed. By taking into account the tradeoff between PSA-Y_{CO2} and PSA-R_{CO2} obtained through modification of the purge mole flow rate, this representation aims to show the range of possible results within the same process framework.

3.1. Number of pressure equalization steps

The cycle adopted in the PSA unit is rather complex. It involves several steps which a single column undergoes and some of these steps imply two different columns to interact. A typical example is the pressure equalization (PEQ) step, where two columns at different pressure levels are put in contact. By means of the pressure gradient, the high pressure column releases part of its bulk gas to pressurize the other. The pressure of the two columns equalizes to a value in the middle between the starting ones. The larger the number of PEQ steps, the larger is the number of columns working in parallel and the more complex becomes the systems. On the other hand, the PEQ steps actively contribute to an efficient separation process, displacing, before regeneration starts, a fraction of the bulk gas that would otherwise leave with CO_2. The correlation between number of PEQ steps, energy and separation performance was studied by running several full-plant simulations. PSA cycles with 4, 3 and 2 PEQ steps were considered, while the general structure of the cycle remains identical. An additional adjustment was introduced to the bed length. Decreasing the number of PEQ steps implies a lower pressure at the beginning of the feed pressurization step and, thereby, a larger amount of gas to pressurize the column. Since the incoming syngas to process is constant, the feed flow rate during the adsorption step would be reduced. For the sake of fair comparisons, we wanted to keep the feed flow rate as stable as possible in the different instances considered. For this reason the length of the column was decreased, down to 9 m and 8 m respectively for the 3PEQ and the 2PEQ case, since this reduces the gas necessary for the column pressurization. **Figure 3** shows the outputs of the simulations implemented. Reducing the number of PEQ steps translates in a decrease of the PSA separation performance, which eventually leads to a decreased η_{CO2}. The η_{el} does not display a clear trend. Its changes result from the balance of CO_2 purity (PSA-Y_{CO2}) and CO_2 recovery (PSA-R_{CO2}) in the PSA process, which both affect the off-gas mass flow rate to be compressed. The number of columns constituting a train and, hence, the footprint of the system is decreasing in accordance with the decrease of the number of PEQ steps implemented. As a general rule, the number of columns needed in the selected process framework is:

$$No.\ \text{columns} = \text{PEQ steps} + 3 \tag{6}$$

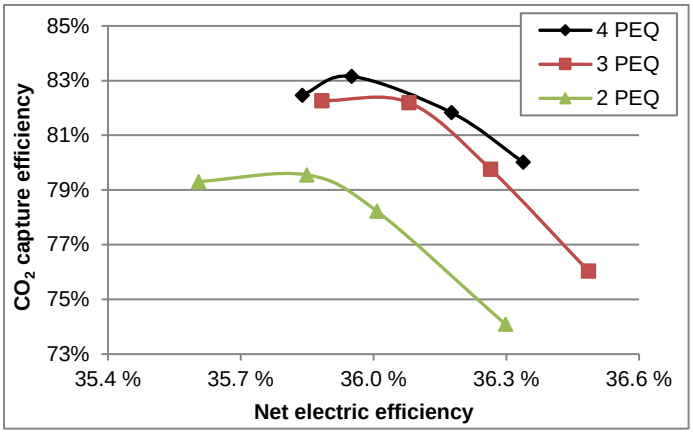

Figure 3. Plant performance with different PEQ steps in the PSA process.

3.2. Regeneration strategy

The modification of the regeneration pressure (P_{reg}) of the PSA process has a direct impact both on the separation and energy performance. The lower the P_{reg} the better is the capacity of the adsorption bed to efficiently desorb CO_2. This translates in higher values of PSA-Y_{CO2} and PSA-R_{CO2}. Conversely, increasing P_{reg} results in a lower effectiveness of the separation process. On an energy point of view, increasing P_{reg} implies a lower pressure ratio for the CO_2 compressor and, hence, a decrease in the power consumption is expected. The system performance was investigated increasing P_{reg} from 1 bar up to 2 and 3 bar. It was decided not to study the effect of P_{reg} lower than 1 bar because that would require the utilization of vacuum pumps, increasing the power consumption and the complexity of the system. Following the same procedure previously outlined, the bed length was adjusted in order to deal with the constraint of processing a fixed syngas flow rate. A higher P_{reg} means that less gas is needed to pressurize the column. Accordingly, the bed length was properly increased to 11 m and 12 m respectively for the P_{reg} 2 and 3 bar case. **Figure 4** shows that an augmented P_{reg} is indeed increasing the η_{el}, as a consequence of the decrease in the CO_2 compressor power consumption. On the other hand the effectiveness of the separation process necessarily decreases and in particular lower PSA-Y_{CO2} values are obtained. The lower the PSA-Y_{CO2}, the higher is the mass flow rate to be compressed. The increased mass flow rate partially counterbalances the reduced pressure ratio in the compressors. However, also the final R_{CO2} (after the flash separation) is decreasing with the increase of P_{reg}, reducing again the mass flow rate to be processed in the final stage of the compression. The overall separation performance is negatively influenced by higher P_{reg}. Whilst the Y_{CO2} remains stable, thanks to the flash separation process, the same is not happening with the R_{CO2}. The increased amount of gas entering the multi-flash unit, due to the lower PSA-Y_{CO2}, makes the flash separation more challenging, resulting in a larger quantity of CO_2 leaving with the H_2-rich gas stream.

In the attempt of limiting the negative effects on the separation efficiency, another regeneration strategy was also tested. It consists in carrying out the regeneration step at different pressure levels. The regeneration pressure (P_{reg}) could be initially fixed to a higher value (e.g., 4 bar) and afterwards to a final atmospheric value. The effectiveness of the bed regeneration should not be heavily influenced by the new process configuration, while the fraction of CO_2-rich gas recovered in the first part of the blowdown would need a lower pressure ratio. Simulations of the PSA process were run with the proposed multi-pressure regeneration step. The pressure levels were set to 4 bar and 1 bar. The PSA process was modified in order to suit the new regeneration procedure (3PEQ steps and different steps time) and the length of the column was set to 11m. The results of the simulations are shown in **Figure**

4. The new regeneration strategy produced a benefit in terms of reduced compressor power consumption in one single case. This is due to the lower PSA-Y_{CO2} we were able to obtain which translated in a larger mass flow rate to be compressed. The maximum energy efficiency achieved (36.4%) is slightly higher than the base case, but to the detriment of the separation performance. The removal of one pressure equalization step is the main reason behind the reduced CO_2 separation efficiency but it is necessary in order to enable a first regeneration step at 4 bar.

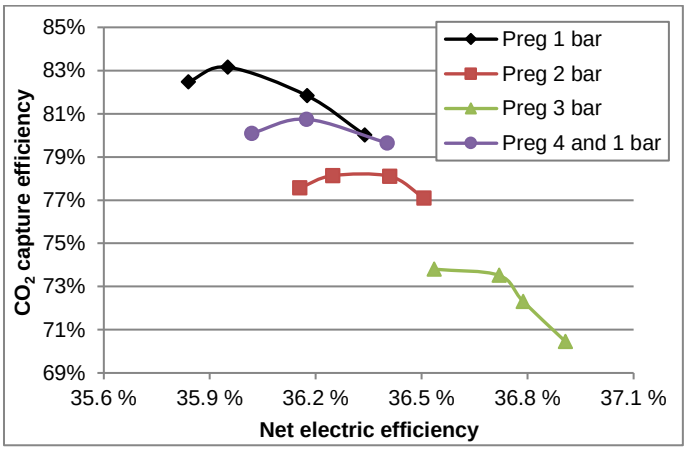

Figure 4. Plant performance with different regeneration strategies.

3.3. Introduction of a heavy-reflux step

A well-documented option to increase the PSA-Y_{CO2} is to introduce a heavy-reflux step in the PSA cycle [22, 23]. It consists in feeding a CO_2-rich stream to the column before blowdown. By means of that, the light-gas, mainly H_2, in the bed void space can be partially displaced. The gas stream utilized to displace the void gas is the product gas obtained from the regeneration process, hence, rich in CO_2. In order to implement the heavy-reflux, the PSA process was redesigned in order to accommodate the new step. It was chosen to set it just before the blowdown, so that it was not needed a significant compression of the product gas to be rinsed. The simulations demonstrate that the addition of a heavy-reflux step is not providing with significant advantages, as can be noticed from **Figure 5**. The obtained increase in the PSA-Y_{CO2} is limited to about 1%. An analysis of the results suggests that the utilization of the rinse gas stream is able to just partially displace the H_2 from the void space of the column. A more complete displacement would require a too large rinse flow rate, which would drastically decrease R_{CO2}. In order to limit the decrease of R_{CO2}, the gas stream leaving the column during the heavy-reflux step is sent to the compression and flash separation unit instead of being vented. The resulting separation performance is on average lower than the base case, while the energy performance registered is on similar levels.

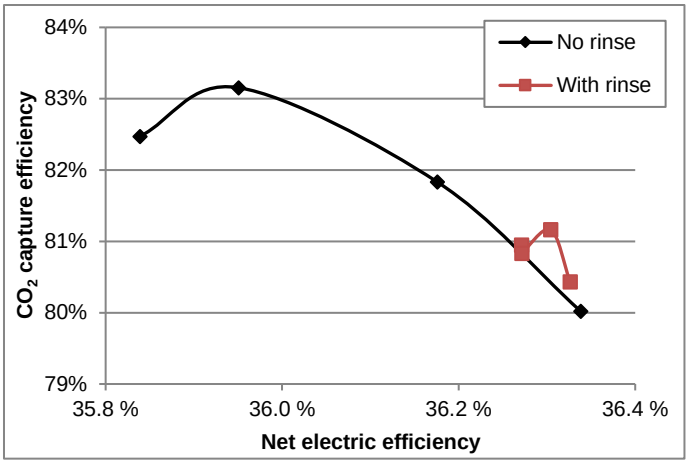

Figure 5. Plant performance with and without a heavy-reflux step in the PSA process.

3.4. Feed temperature

The temperature adopted at the entrance of the PSA unit (T_{feed}) has an impact on the plant performance. This effect has been evaluated by simulating the plant behavior at different T_{feed}: 328 K, 338 K (base case), 348 K, 358 K and 368 K. In the first instance, it is interesting to notice the effect on the separation unit (see **Figure 6**). One would expect the PSA process to perform better at the lowest temperature tested, in accordance with the exothermic nature of adsorption. Conversely, the actual trend is showing a maximum in the separation performance (CO_2 purity and recovery for the PSA process) when the T_{feed} is set to 348K. In order to explain this trend, the whole cycle needs to be taken into consideration. Whilst low temperatures are beneficial for adsorption (exothermic process), they are detrimental for desorption (endothermic process and because the adsorbent saturate at lower pressures). In the PSA process investigated, no temperature swing is implemented. Thus, the lower is the temperature at the beginning of the cycle, the lower will likely be during the regeneration steps. The working capacity, defined as the difference between the equilibrium capacity during adsorption and desorption, constitutes the real measure of the effectiveness of the separation process. It reached a maximum when the syngas is introduced at 348K. It has been shown before that not always the optimum for the PSA unit corresponds to the optimum for the overall plant. The full-plant model allowed the investigation of the T_{feed} effect also at a system level. The base case with a P/F ratio of 0.14 was selected as starting point and the different T_{feed} were tested. The outputs of the simulations are shown in **Figure 7**. The best cases on a CO_2 separation point of view (T_{feed} 348K and 358K) display a small decrease in the η_{net}. This is due to two main factors: the higher CO_2 recovery, which implies a larger gas stream to be compressed, thereby increased power to the compressors (even though also the CO_2 purity is increasing, partially counterbalancing that); the slight less efficient H_2 recovery in the flash separation unit and the consequent decrease of the gross power output. In spite of that, they are more effective than the other cases assessed (T_{feed} 328K and 368K) which achieve slightly lower energy penalty at the expense of more significant reduction of the CO_2 separation efficiency.

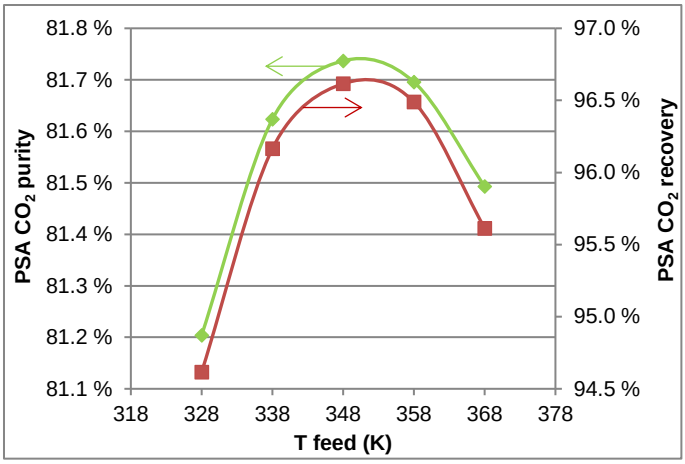

Figure 6. PSA performance with different T_{feed}.

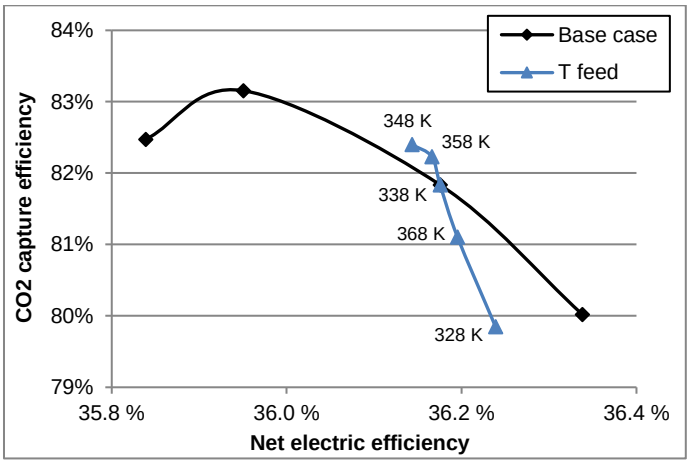

Figure 7. Plant performance with different T_{feed}.

3.5. Flash pressure

The CO_2-rich product stream which is leaving the PSA unit is sent to the CO_2 compression and flash separation unit. There a first compression process increases the pressure before the gas stream enters two multi-stream heat exchangers and two flash separators. The operating parameters were set according to previous studies and taking into account thermodynamic constraints to the system [24-26]. This section wants to investigate the impact of modification of the flash pressure P_{flash} (i.e., the pressure after the first compression, at which the gas stream enters the first flash column). The base case sets it to 30 bar. Two additional pressure levels were considered, namely 28 bar and 26 bar. Lower pressures were not considered because the H_2 recovered in this process is sent to the gas turbine and needs to have a pressure of about 24 bar. Considering the pressure drops in the unit, the P_{flash} cannot be set lower than 26 bar, unless a recompression is planned. The outputs of the simulations are shown in **Figure 8**. The general trend is that decreasing P_{flash} has a negative effect on the separation performance. The separation in the flash columns becomes less effective and the CO_2 recovery decreases (hence also η_{CO2}). However, a large fraction of H_2 is still recovered (more diluted with CO_2) and the overall compression power decreases. Thus, the η_{net} is slightly lifted up.

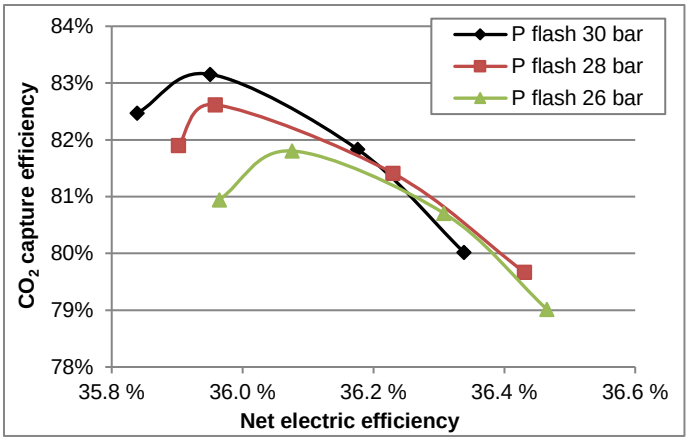

Figure 8. Plant performance with different P_{flash}.

3.6. *CO_2 recirculation*

A way to improve the CO_2 separation process is to recirculate part of the product CO_2-rich stream and increasing the CO_2 partial pressure entering the PSA unit. This possibility is analysed by utilizing CO_2 as fuel preparation gas (an option already proposed in the literature [27]). The coal feeding system is normally designed to utilize 0.02207 kg N_2 per kg coal, with the pure N_2 taken from the ASU. If CO_2 has to be used, the gas flow rate required is double than the flow rate of N_2 and the operating conditions need to be adjusted [16]. The CO_2 used in the fuel feeding system is extracted from the CO_2 compression section at a pressure of 50bar, as requested by the specifications. **Figure 9** shows the results obtained by the full-plant simulations. Better separation performance was obtained. With a sufficiently high P/F ratio the R_{CO2} reaches the desired level of 90%, while the Y_{CO2} remains on high levels (>99%). The increase in η_{CO2} is more limited as it reaches a maximum value of 85%. In fact, the enhanced separation performance is counterbalanced by an increase in the energy penalty. Since the amount of the gas stream needed for transporting the coal is double than the N_2-based counterpart, the amount of gas to be processed is increased. This translates into augmented power consumption for the compressors which have to compress a larger mass flow rate. Another modification observed is that the steam turbine power output slightly decreases because a larger quantitative of steam needs to be extracted to be fed to the WGS process, due to the larger fraction of CO in the syngas. These two effects outbalance the power consumption reduction in the ASU, due to the missing N_2 compression for fuel preparation purposes. The overall outcome is that the energy efficiency is reduced to values between 35.0 and 35.7%.

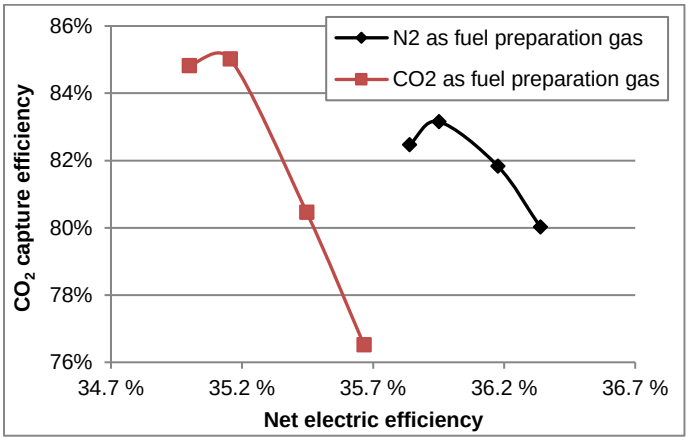

Figure 9. Plant performance with and without CO_2 recirculation.

3.7. *Remarks on the process configuration and operating conditions analysis*

Figure 10 shows the performance of the base case defined, all the simulation outputs of alternative process configurations and the reference results for absorption. It is interesting to look at the overall trend represented in the figure. The base case is an acceptable compromise between energy and separation efficiency. Enhancements can be achieved by modifications of the process configuration or of its operating parameters. However, most of the times, an improvement in the energy efficiency results in a decrease of the CO_2 capture efficiency (e.g., increasing P_{reg}) and vice versa (e.g., CO_2 recirculation). Consequently, it is difficult to state what is the optimum process configuration or set of operating parameters. Those are dependent on the specific requirements the plant needs to fulfil. So, for example, if a CO_2 recovery of about 80% was considered acceptable, some of the configurations studied would return η_{el} on the level of the absorption counterpart. A certain flexibility in the range of performances achievable is to be noted. However, **Figure 10** clearly shows that modifications to the process may fill the gap with absorption only in relation to a specific performance indicator. When the effectiveness of the separation technologies is analysed as a whole (energy, separation and footprint), absorption is still displaying an advantage over PSA.

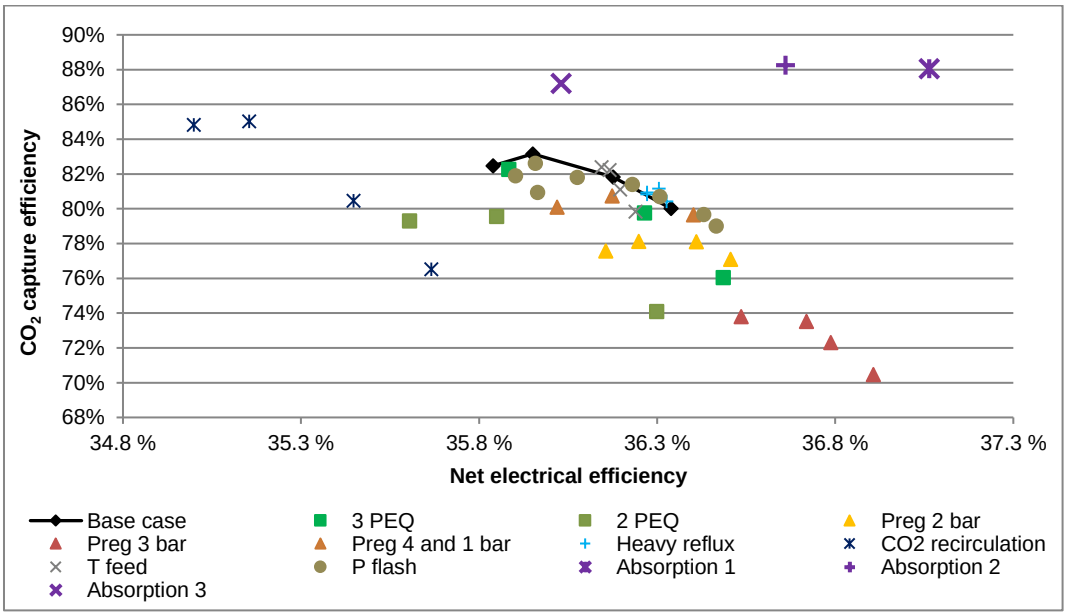

Figure 10. Overview of plant performances achievable by modifications of the process.

4. Adsorbent material

The characteristics of the adsorbent material have a strong impact on the effectiveness of the CO_2 separation process. One of the firsts and more important decisions when it comes to design a PSA process is the choice of the proper adsorbent. In the previous analyses the adsorbent considered is a commercial activated carbon [18]. Activated carbon demonstrates to outperform zeolites (which are normally considered to be the benchmark for CO_2 separation) when the adsorption process occurs at relatively high CO_2 partial pressure [28]. This is the case for a pre-combustion application. Other advantages of activated carbons over zeolites are the lower costs [8] and the higher resistance to water presence in the gas mixture [8, 29, 30]. Material science is very active in the research of new adsorbents with enhanced characteristics for CO_2 separation [31-34]. Much effort is put in the laboratory tests to

develop adsorbents with remarkable performance. In this section a different approach has been adopted for the study of adsorbent materials influence. Instead of testing specific adsorbents, which would require the availability of a large amount of modeling data, we tried to define the optimum characteristics of an adsorbent to perform efficiently in the framework under investigation. Taking as reference the activated carbon, a sensitivity analysis on some meaningful properties was carried out. The original values of the properties were varied in targeted ways in order to evaluate how those variations affect the process performance, and to pinpoint the most influential properties. The output variables carefully monitored were those related to the effectiveness of the adsorbent. It was taken track of the effects on the CO_2 recovery, purity and on the selectivity at which the material is able to separate CO_2. The full-plant model enabled then to assess the impact on the overall system. Being aware of the limitations of such analysis, it was thought to be useful for providing an indication on the performance enhancements realistically achievable by advancements in the adsorbent materials. Furthermore, it can be a source of inputs and guidelines to the material scientists in order to address future developments.

4.1. *Sensitivity analysis*

The equilibrium behavior of the activated carbon is described by a multi-site Langmuir isotherm [35]:

$$\frac{q_i^*}{q_{m,i}} = a_i k_i P_i \left[1 - \sum_i^{NC} \left(\frac{q_i^*}{q_{m,i}} \right) \right]^{a_i} \quad \text{, with } \; k_i = k_{\infty,i} \exp\left(-\frac{\Delta H_{r,i}}{RT} \right) \tag{7}$$

The values of the properties have been taken from the literature [18] and they are shown in **Table 3**.

Table 3. Adsorption and physical properties of the reference activated carbon.

Activated carbon and adsorbent bed - Physical properties						
	d_p (mm)	ε_p	ρ_p (kg/m^3)	$C_{p,s}$ (J/kg/K)	ε	
	2,34	0,57	842	709	0,38	
Activated carbon - Equilibrium and kinetic parameters						
	a (-)	k_∞ (Pa^{-1})	q_m (mol/kg)	ΔH_r (kJ/mol)	D_{0c}/r_c^2 (s^{-1})	Ea (kJ/mol)
CO_2	3,0	2,128E-11	7,855	-29,1	17,5	15,8
N_2	4,0	2,343E-10	5,891	-16,3	1,0	7,0
H_2	1,0	7,690E-11	23,570	-12,8	14,8	10,4
CO	2,6	2,680E-11	9,063	-22,6	59,2	17,5

An ideal adsorbent selectively retains CO_2 on its surface while the other components are flowing through. However, in a real process a fraction of all the non-CO_2 components is also fixed on the solid surface. An adsorbent can be improved according to two different strategies: its ability of fixing CO_2 can be increased or the undesired uptake of the other gas components can be decreased. Accordingly, the properties have been divided into two groups: the CO_2-related properties on one side, the properties of non-CO_2 components (i.e., H_2, CO and N_2) on the other. When the impact of one CO_2 property (e.g., $q_{m,CO2}$) had to be evaluated, its value was increased in fixed percentages (+ 1%, 5%, 10%, 20%, 30%), while the values of all the other properties were kept constant. Conversely, when the impact of a non-CO_2 property was investigated (e.g., $q_{m,non\text{-}CO2}$), only the values of that property referring to the non-CO_2 components were decreased to the same extent (- 1%, 5%, 10%, 20%, 30%). The properties selected for the study are:

- the *maximum adsorption capacity* q_m, indicating the maximum amount of the specific component that can be adsorbed per kg of adsorbent.
- the *adsorption equilibrium constant at infinite temperature* k_∞, necessary for calculating the adsorption equilibrium constant k.
- the *isosteric heat of adsorption* ΔH_r, measuring the strength of adsorption of the specific component to the adsorbent.

The material and packing characteristics were also taken into account in the analysis, in the form of void fractions. They were expected to have a significant influence on the performance of the adsorption process. In the first instance because they affect the volume based adsorption capacity of the bed. Furthermore, it was noticed that a significant fraction of the impurities leaving with CO_2 rather than being adsorbed onto the solid - and released during bed regeneration - are accumulated in the void spaces of the bed as bulk phase. Thus, reducing the void space is expected to reduce the accumulation of impurities in the bed. The void fraction was considered at two levels, which were decreased of - 1%, 5%, 10%, 20%:

- the *particle void fraction* ε_p, measuring the void space in the particle due to its porous structure.
- the *bed void fraction* ε, measuring the void space in the bed due to the characteristic of the packing.

An example can be useful to clarify the procedure. Assuming that $q_{m,CO2}$ is the property to be investigated, its original value 7.885 mol/kg is increased of the mentioned percentages. The physical meaning of this is that a kilo of the adsorbent can accommodate at equilibrium a larger amount of CO_2. The value of the all the other properties is unvaried. When the same analysis is to be done on the $q_{m,non\text{-}CO2}$, the maximum capacity of H_2, CO and N_2 are decreased according to the selected percentages (meaning that a kilo of adsorbent can accommodate at equilibrium a lower amount of those components). The other properties are at the reference value, included $q_{m,CO2}$. The same procedure was utilized to study all the properties. This methodology allows evaluating the influence of each single property studied, given that any variation in the performance can be uniquely ascribed to the implemented modification.

4.2. *Effect on the PSA process*

The effect of the sensitivity analysis was first evaluated on the separation effectiveness of the PSA process. The output is graphically shown in **Figure 11**, **Figure 12**, **Figure 13** and **Figure 14**. The horizontal axis indicates the extent of the modification implemented on the single property, while on the vertical axis the CO_2 purity or recovery obtained by means of that modification is reported. As we described, the CO_2 properties were increased of fixed percentages, while the non-CO_2 properties were decreased to the same extent. A base case performance is reported, where the characteristics of the PSA cycle are those previously outlined (*cf.* 2.2 *Base process conditions and specifications*). Since the purity appeared to be the most critical factor, it was chosen to use as starting point for the sensitivity analysis one with a low P/F ratio (i.e., P/F = 0.06) which returns the following results: PSA-Y_{CO2} = 85.3% and PSA-R_{CO2} = 88.7%. Such choice was taken in order to be able to ascribe any further increase of the purity to the material modification and not to the trade-off of some percentage points of the recovery.
All the modifications proposed tend to increase both CO_2 recovery and purity. This was expected since the way to vary the properties was meant to improve the adsorbent material. Different properties show different influences on the separation efficiency. ΔH_r seems to display the strongest one. An increase of $\Delta H_{r,CO2}$ brings a positive effect on the isotherm at high pressure. Contemporary the adsorption isotherm becomes steeper in the low pressure region, thus it becomes more and more difficult to desorb CO_2 from

the bed. For small increases of $\Delta H_{r,CO2}$ the overall effect is positive (the working capacity is augmented). For higher values of $\Delta H_{r,CO2}$, the reduced effectiveness of the regeneration process starts to prevail. Accordingly, the positive effect reaches a maximum when the value is increased of about 10%; after that, the benefits on the performance indicators tends to diminish. When the decrease of $\Delta H_{r,non\text{-}CO2}$ is considered, the uptake capacity for non-CO_2 components at high pressure is reduced; hence a lower amount of those gases is retained on the material during adsorption step and a higher amount of CO_2 can be fixed, with a consequent benefit on CO_2 recovery. Furthermore, decreasing the strength of the adsorption bond for the non-CO_2 components (i.e., reducing $\Delta H_{r,non\text{-}CO2}$) makes their regeneration easier. A large fraction of them can be desorbed during the PEQ steps, which become extremely effective and avoid a drastic reduction of PSA-Y_{CO2}.

Also $q_{m,CO2}$ has a strong impact on the separation process. An increase of $q_{m,CO2}$ results in a remarkable increase of PSA-R_{CO2} (on the same level attained with modification of ΔH_r) because of the increased uptake capacity of the adsorbent. On the other hand, the PSA-Y_{CO2}, after an initial increase, drops to values lower than the base case. This is due to the CO_2 adsorption wavefront getting steeper for the higher driving force exercised by the adsorption bed. Accordingly, the part of the bed not saturated with CO_2 adsorbs a higher amount of the other components, whose adsorption wavefront travels quicker through the column. Those components are then released during desorption producing the reduction of PSA-Y_{CO2}.

The other properties examined (i.e., $q_{m,non\text{-}CO2}$ and $k_{\infty,CO2}$ and $k_{\infty,non\text{-}CO2}$) display a similar, more limited, effect. The performance indicators increase in an almost linear way but more slowly than the previous cases. Reducing $q_{m,non\text{-}CO2}$ increases the active sites available for CO_2 uptake and the reduction of the non-CO_2 components adsorbed is also beneficial for the regeneration process. Modifications in k_∞ – whether increasing $k_{\infty,CO2}$ or decreasing $k_{\infty,non\text{-}CO2}$ – act as correspondent modifications in the partial pressure. Thereby, they have a steady positive effect increasing with the extent of the modification.

The last parameters analysed were ε_p and ε. Their trend is similar even though ε_p displays a stronger impact, both positive and negative, on the separation performance. The implemented reduction of the void fractions has as primary effect the increase of the adsorbent and bulk density. A larger quantity of adsorbent can be accommodated per volume of bed, thus more CO_2 can be fixed. This explains the remarkable increase in the PSA-R_{CO2}. A diminished void fraction reduces also the amount of bulk gas accumulated in the bed. Given that such bulk gas is mainly constituted by the lighter components, H_2 in the first instance, and that they are released during the regeneration steps, an initial increase of PSA-Y_{CO2} can be verified. However, when the decrease of the void fractions exceeds certain levels, the amount of non-CO_2 components retained onto the adsorbent augments so much, due to the increased adsorbent and bulk densities, to overcome the reduction of impurities present as bulk phase. The PSA-Y_{CO2} starts then to decrease significantly.

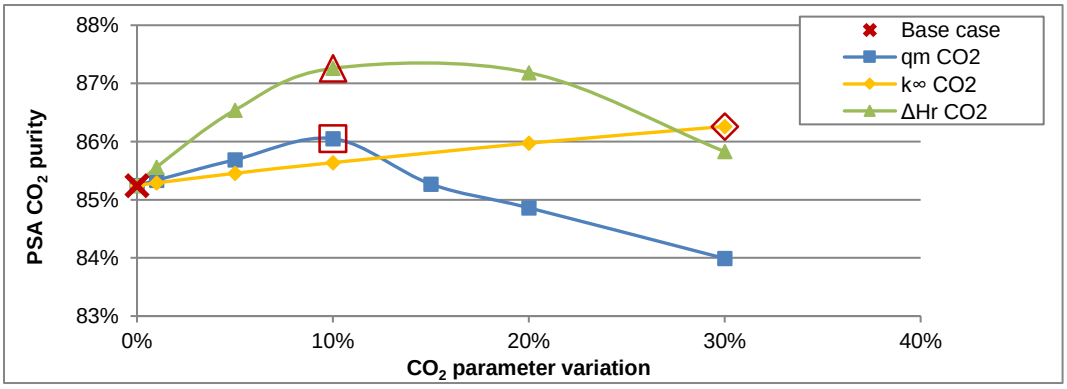

Figure 11.Effect on the PSA CO2 purity of the sensitivity analysis on the CO_2 related properties.

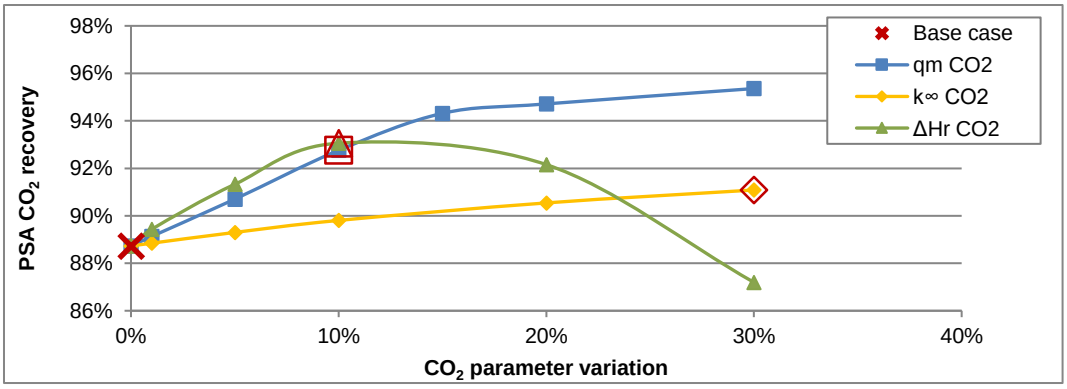

Figure 12. Effect on the PSA CO_2 recovery of the sensitivity analysis on the CO_2 related properties.

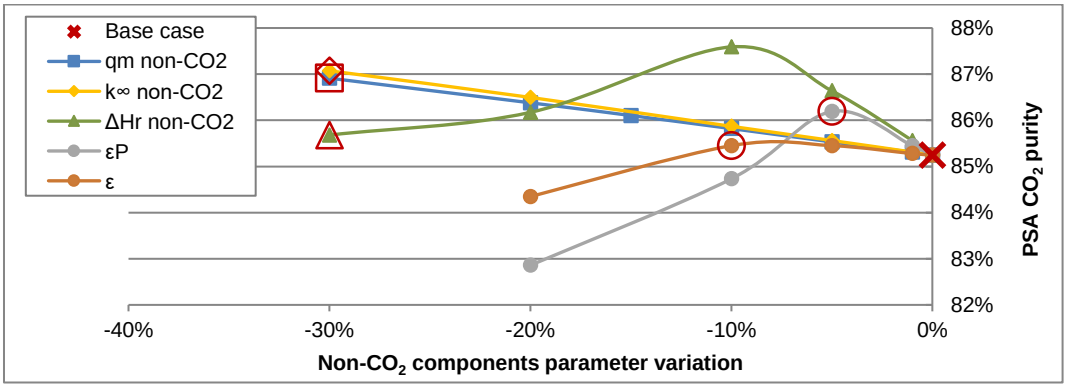

Figure 13. Effect on the PSA CO_2 purity of the sensitivity analysis on the non-CO_2 related properties.

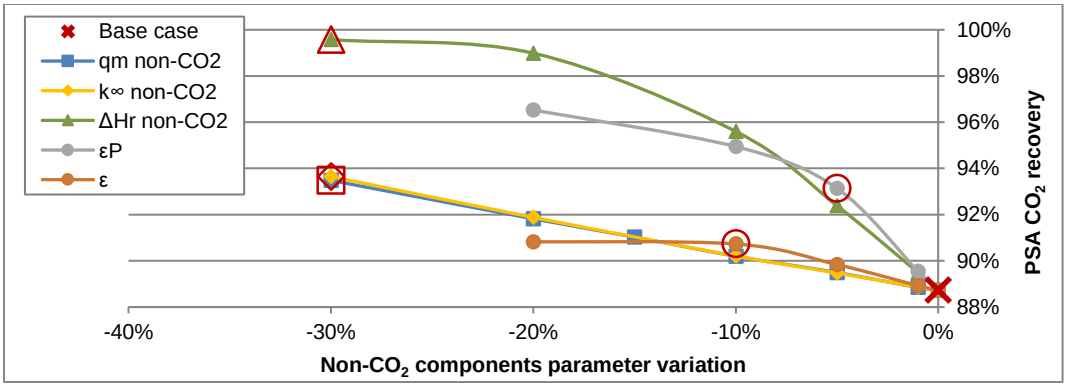

Figure 14. Effect on the PSA CO_2 recovery of the sensitivity analysis on the non-CO_2 related properties.

4.3. *Effect on the overall plant*

In order to evaluate the overall effect on the plant, the most significant cases were extrapolated by the previous analysis (highlighted in the previous figures) and utilized in the full-plant model. It was chosen to select one example for each type of property variation studied. The instances selected are listed hereafter and can be thought as fictitious adsorbents with improved characteristics:

- $q_{m,CO2}$ +10%
- $q_{m,non\text{-}CO2}$ -30%
- $k_{\infty,CO2}$ +30%
- $k_{\infty,non\text{-}CO2}$ -30%

- $\Delta H_{r,CO2}$ +10%
- $\Delta H_{r,non\text{-}CO2}$ -30%
- ε_p -5%
- ε -10%

Two additional cases are also proposed. They consider the contemporary modification of a group of properties, rather than of a single one. The aim was to verify if the positive effects of the implemented modifications could be combined. The two cases studied refer to fictitious adsorbents with the following characteristics:

- Combined 5: $q_{m,CO2}$ +10%, $k_{\infty,CO2}$ +10%, $\Delta H_{r,CO2}$ +10%.
- Combined 6: $q_{m,non\text{-}CO2}$ -10%, $k_{\infty,non\text{-}CO2}$ -10%, $\Delta H_{r,non\text{-}CO2}$ -10%.

The output of the simulations, in terms of CO_2 capture efficiency and net electric efficiency, are shown in **Figure 15**. The absorption-based results are also included. Likewise the process analysis, the base case is represented as a line and not as a single point. The line is draw by connecting different base case points. Those instances refer to the unmodified activated carbon material with different P/F ratios in the PSA process. This representation is useful because it helps to point out the performance improvements effectively ascribable to the material. A process modification as simple as increasing the purge flow rate in the PSA process is able to tradeoff part of the PSA-Y_{CO2} for a higher PSA-R_{CO2}, with consequences on the full-plant performance. The base case line takes into account this effect and sets the benchmark for our analysis. If a simulation output produces a point which lies above the base case line, the correspondent case can claim to bring an actual performance improvement, regardless the process influence. All the cases reported fall in this category. Also the simulations referring to combined property modifications were run for different P/F ratios.

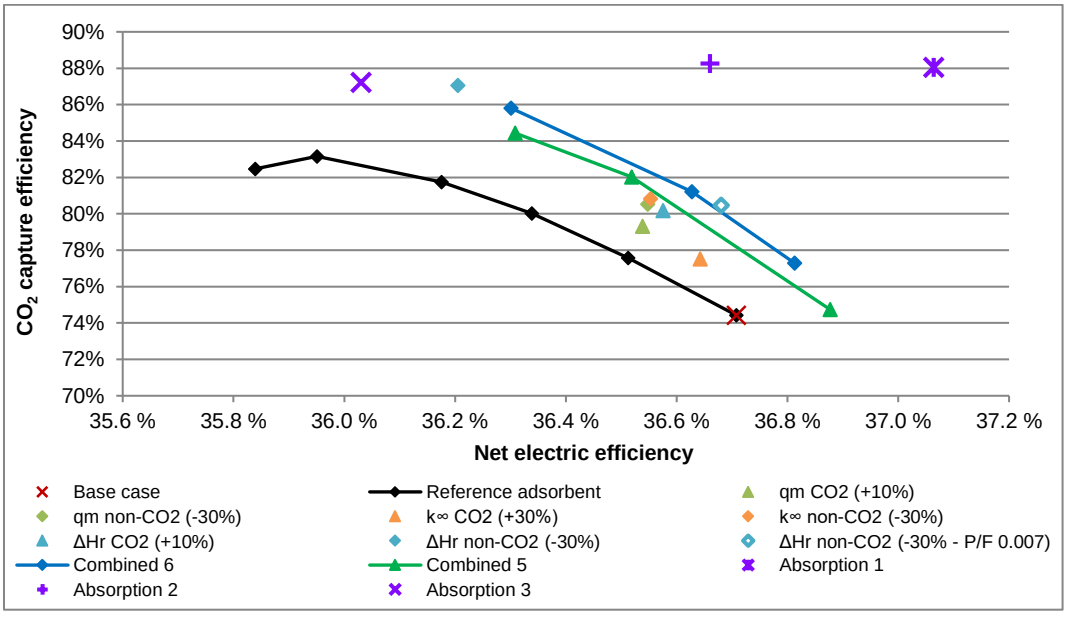

Figure 15. Overview of plant performances achievable by modifications of the material.

4.4. *Remarks on the adsorbent material analysis*

It has been demonstrated that proper modifications of the adsorbent specific properties can bring significant performance improvements. Some of these material properties displayed a stronger impact on the separation process and, consequently, on the overall process. This is the case of the heat of reaction of non-CO_2 components ($\Delta H_{r,non\text{-}CO2}$). Its reduction demonstrated to bring significant benefits, standing out among the other results obtained. The case simulated (i.e., $\Delta H_{r,non\text{-}CO2}$ -30%) achieves a η_{CO2} (87.1%) which is comparable to that of an absorption-based plant, even though the η_{el} still ranks slightly lower. A higher value for η_{el} can be obtained by exploiting the influence of the process. An example is reported, where the same modified adsorbent ($\Delta H_{r,non\text{-}CO2}$ -30%) is used adopting a lower P/F ratio (P/F = 0.007) in the PSA process. The empty diamond in **Figure 15** is showing the relative full-plant simulation output. It can be noted that, whilst the η_{CO2} decreases down to 80.5%, the η_{el} can be lifted up to 36.7%, a value which is competitive with absorption. Similar results are obtained by combined modifications of the properties, especially for the case involving all the non-CO_2 properties reduced of 10% (i.e., Combined 6). This is leading to another interesting remark. The properties modifications which reduce the material affinity for non-CO_2 components seem to be more effective than those increasing the CO_2 adsorption properties. This can be verified both on the single property modification (diamonds are generally located over triangles in **Figure 15**) and in the two combined modification examples (Combined 6 performs better than Combined 5). This trend highlights the importance to focus not only on the CO_2 adsorption characteristics when developing an adsorption material. In order to guarantee a good selectivity for the gas separation process, it is fundamental also to assure that the uptake of the non-desired gases is limited. Summing up, tailored advancements in the adsorbent material demonstrated to be potentially very important to increase the competitiveness of PSA. The cases analysed, even though based on arbitrary property modifications, shows that the development of improved adsorbents may substantially reduce the gap with absorption. Even though some criteria are indicated in order to guide this development, it is beyond the scope of this work to define how to pursue them. What can be mentioned is that a variety of activated carbons can be produced, allowing tailoring of their adsorptive properties. Even more promising is the utilization of Metal Organic Frameworks (MOFs). Their structure and chemical composition can be easily tuned in order to obtain desired properties. It must be also pointed out that the analysis carried out covers only the adsorbents with a Langmuir-like shape isotherm. This family of adsorbents encompasses, among others, activated carbons and some MOFs. Other MOFs display a sigmoidal shape which could lead to different performance. However, additional research efforts need to be carried out to guarantee the actual applicability of MOFs. The main issues yet to be addressed are related to the effect of impurities, the practical aspects of employing a PSA process [36], the stability over multiple adsorption/desorption cycles [8], the material formulation and mechanical stability [32].

5. Synergies between process and adsorbent material

In the previous sections advancements of the process and of the material were investigated in order to enhance the overall plant performance. However, the approach adopted is to some extent inaccurate. It considers the two domains as separated issues, while they have a strong influence on each other. It should be good practice to deal with the plant optimization problem as a whole. Such way of proceeding complicates the analysis but reveals synergies that can be very beneficial. Therefore an attempt in this sense was made by trying to define an optimal adsorbent for a specific process configuration.
The PSA process taken into account was meant to return a good performance under an energy point of view. Utilizing the knowledge acquired, the process configuration was designed with the following changes compared to the base case:

- P_{reg} 2 bar
- T_{feed} 358 K
- P_{flash} 26 bar.

The following step was to determine the adsorbent properties modifications which would make the adsorbent to perform efficiently in this new set of operating conditions. The exact definition of the most suitable properties values is not an easy task, as the PSA process is influenced by a large number of parameters. The methodology to determine which properties to modify, how and to what extent was based on the experience gained with the previous analysis on the material adsorbent. However, it also relied to some degree on a trial and error procedure. The outcome was a modified adsorbent with the following characteristics:

- $q_{m,CO2}$ and $k_{\infty,CO2}$ + 10%
- $\Delta H_{r,CO2}$ -10%
- $q_{m,non\text{-}CO2}$ and $k_{\infty,non\text{-}CO2}$ and $\Delta H_{r,non\text{-}CO2}$ -30%

The CO_2 heat of adsorption was decreased of 10%. The explanation for that should be searched in the effect of ΔH_r on the slope of the adsorption isotherm. In order for the regeneration process to be effective at a higher pressure (i.e., P_{reg} 2 bar), the slope of the adsorption isotherm needs to be gentler in the low pressure region. A decrease of ΔH_r works in that way. Without further changes, the decrease of ΔH_r would also reduce the CO_2 uptake at high pressures, hindering the adsorption process. Thereby, $q_{m,CO2}$ and $k_{\infty,CO2}$ were increased to restore the adsorption capacity during the adsorption step. This increase was limited to 10% because further increases demonstrated to be ultimately ineffective. Additionally, all the properties relative to the non-CO_2 components were decreased of 30% as it demonstrated to be beneficial (*cf*. 4.2 Effect on the PSA process).
The new defined scenario, involving a material with tailor-made characteristics for the chosen process configuration, was named *Synergy* and it was simulated for three different P/F ratios. The outputs are displayed in **Figure 16**. The obtained energy performance are extremely competitive (with values between 36.8% and 37.1%) and on average higher than those achievable with absorption. The CO_2 capture efficiency still ranks lower than the absorption-based counterpart, as it ranges between 76% and 82%, but it was not dramatically reduced. **Figure 16** shows also all the outputs obtained by process modifications (squares) or material modifications (triangles) and discussed in previous sections. It is worthwhile to notice that the approach adopted seems to add together the benefits achieved by the two domains subject of our analyses. This example demonstrates how the close collaboration between process engineering and material science is of paramount importance in order to develop effectively the studied system. Even though the proposed case is based on a fictitious adsorbent material, the general remark could be that there is room for improvements and for approaching competitiveness in the pre-combustion scenario.

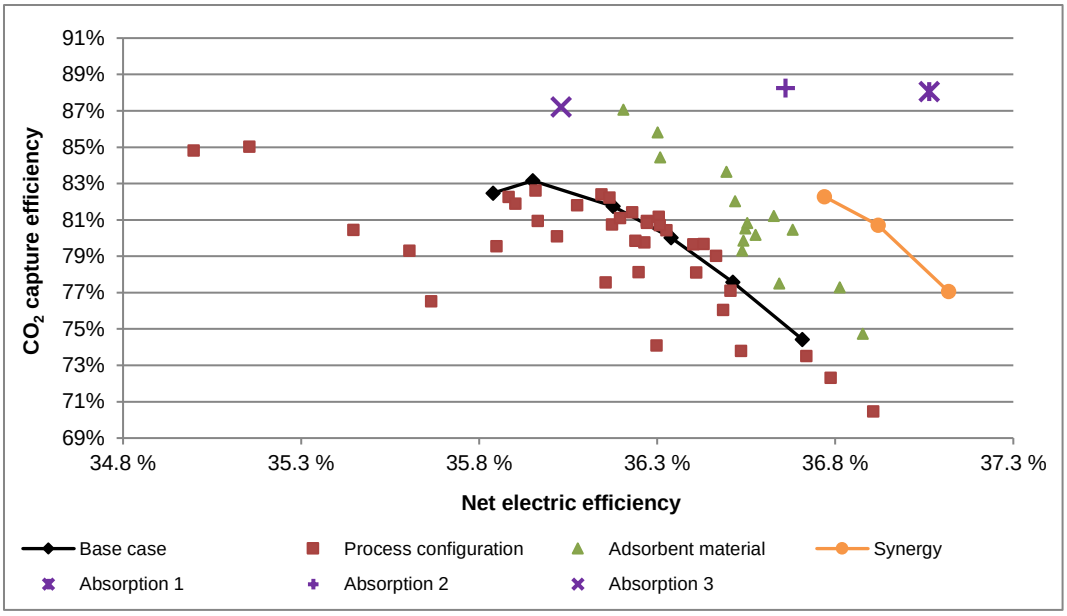

Figure 16. Plant performance achieved through a synergetic approach of process and material modifications. All the performances achieved by modification of the process or the material are also reported.

6. Conclusions

An analysis on the feasibility and competitiveness of PSA in a pre-combustion CO_2 capture application has been carried out. The system considered for the analysis is an IGCC plant. The plant integrating a PSA unit has been defined and a composite model has been built in order to simulate its functioning. The performances obtained, evaluated in terms of energy and CO_2 separation efficiency, are compared to state-of-the-art absorption-based plants. The range of performance and the potential of the IGCC-PSA system were investigated by taking into consideration two domains, which were thought to have a significant influence: the process configuration and the adsorbent material.

Different process configurations and operating conditions were studied through process simulations. Such analysis improved the understanding of the system, enabling a correct evaluation of the available options for boosting the plant performance according to specific requirements. A tradeoff between energy efficiency and CO_2 separation efficiency was observed. Competitive energy penalty could be obtained, at the expense of substantial reduction of the CO_2 capture efficiency. The optimum plant configuration is difficult to be defined without establishing which performance indicator to prioritise and which performance levels are acceptable. None of the options studied could fully fill the performance gap with regard to absorption.

The influence of the adsorbent material on the overall plant performance was studied through a sensitivity analysis. Given an activated carbon as reference adsorbent, the impact of improved adsorption properties was studied by varying them in a targeted manner and thus simulating advancements in the material. The objective was to establish the most influencing properties, to assess the possible performance enhancements and to provide guidelines for future material development. The effects were first evaluated on the separation process. The effects on the final CO_2 recovery, purity and on the selectivity at which the material is able to separate CO_2 were monitored. The most significant cases resulting from this analysis were implemented in the full-plant model, in order to assess the impact on the overall plant. The material modifications proposed demonstrated to enhance the system performance, albeit not on the level of absorption. Some adsorbent properties showed a stronger impact than others. It was also noticed that decreasing the adsorbent affinity for non-CO_2 components seems

slightly more effective than increase its affinity towards CO_2. Proper advancements in the adsorbent materials have the chance to give an important contribution to boost PSA competitiveness.
The last analysis proposed aims to combine the positive effects obtained by modifications in the process and in the adsorbent material. An attempt was made in order to exploit possible synergies, utilizing the knowledge acquired in the previous analyses. A material tailor-made on a specific process configuration was defined. The performance resulting from the process simulation was extremely promising. A net electric efficiency slightly higher than the reference absorption value could be obtained, without large reduction in the CO_2 capture efficiency. A synergy of process engineering and material science demonstrated to be a key issue for enhancing PSA competitiveness.

Acknowledgements

The authors gratefully acknowledge the financial support provided through the "EnPe – NORAD's Programme within the energy and petroleum sector".

Nomenclature

a_i	number of neighboring sites occupied by adsorbate molecule for species i
$C_{p,s}$	particle specific heat at constant pressure, J/(kg • K)
$D_{0c,i}$	limiting micropore diffusivity at infinite temperature of species i, m^2/s
d_p	particle diameter, m
$E_{a,i}$	activation energy of species i, J/mol
$\Delta H_{r,i}$	isosteric heat of adsorption of species i, J/mol
k_i	equilibrium constant of species i, Pa^{-1}
$k_{\infty,i}$	adsorption constant at infinite temperature of species i, Pa^{-1}
P	pressure, Pa
P_{flash}	pressure at the entrance of the flash column, bar
P_{reg}	regeneration pressure for the PSA process, bar
q_i^*	equilibrium adsorbed concentration of species i, mol/kg
$q_{m,i}$	maximum adsorption capacity of species i, mol/kg
R	universal gas constant, Pa • m^3/(mol • K)
R_{CO2}	CO_2 recovery
R_{H2}	H_2 recovery
t	step time, s
T	temperature, K
T_{feed}	temperature at the entrance of the PSA column, K
Y_{CO2}	CO_2 purity

Greek letters

ε	bed void fraction
ε_p	particle void fraction
η_{CO2}	CO_2 capture efficiency
η_{el}	net electric efficiency
ρ_p	volumetric mass density of the particle, kg/m^3

Acronyms

CCS	carbon capture and storage

CSS cyclic steady state
DHU dehydration unit
FS flash separator
HRSG heat recovery steam generator
IGCC integrated gasification combined cycle
LHV lower heating value
NC number of components
PEQ pressure equalization
P/F purge-to-feed
PSA pressure swing adsorption
SEWGS sorption enhanced water gas shift
WGS water gas shift

References

1. IEA, *Energy and Climate Change - World Energy Outlook Special Report*, 2015.
2. IEA, *Technology Roadmap - Carbon capture and storage*, 2013.
3. Institute, G.C., *The Global Status of CCS: 2014*, 2015.
4. Khoo, H.H. and R.B.H. Tan, *Life Cycle Investigation of CO2 Recovery and Sequestration.* Environmental Science & Technology, 2006. **40**(12): p. 4016-4024.
5. Abanades, J.C., et al., *Emerging CO2 capture systems.* International Journal of Greenhouse Gas Control, (0).
6. Ebner, A.D. and J.A. Ritter, *State-of-the-art Adsorption and Membrane Separation Processes for Carbon Dioxide Production from Carbon Dioxide Emitting Industries.* Separation Science and Technology, 2009. **44**(6): p. 1273-1421.
7. Reynolds, S.P., A.D. Ebner, and J.A. Ritter, *Stripping PSA Cycles for CO2 Recovery from Flue Gas at High Temperature Using a Hydrotalcite-Like Adsorbent.* Industrial & Engineering Chemistry Research, 2006. **45**(12): p. 4278-4294.
8. Choi, S., J.H. Drese, and C.W. Jones, *Adsorbent materials for carbon dioxide capture from large anthropogenic point sources.* ChemSusChem, 2009. **2**(9): p. 796-854.
9. Riboldi, L. and O. Bolland, *Evaluating Pressure Swing Adsorption as a CO2 separation technique in coal-fired power plants.* International Journal of Greenhouse Gas Control, 2015. **39**(0): p. 1-16.
10. Liu, Z. and W.H. Green, *Analysis of Adsorbent-Based Warm CO2 Capture Technology for Integrated Gasification Combined Cycle (IGCC) Power Plants.* Industrial & Engineering Chemistry Research, 2014. **53**(27): p. 11145-11158.
11. Gazzani, M., E. Macchi, and G. Manzolini, *CO2 capture in integrated gasification combined cycle with SEWGS – Part A: Thermodynamic performances.* Fuel, 2013. **105**(0): p. 206-219.
12. Najmi, B., O. Bolland, and K.E. Colombo, *Load-following performance of IGCC with integrated CO2 capture using SEWGS pre-combustion technology.* International Journal of Greenhouse Gas Control, 2015. **35**(0): p. 30-46.
13. Baade, W., et al., *CO2 capture from SMRs: A demonstration project.* Hydrocarbon Processing, 2012: p. 63-68.
14. *Thermoflex Version 24.0.1*, 2014, Thermoflow Inc.
15. *gPROMS* 2012, Process System Enterprise Limited.
16. *DECARBit: Enabling advanced pre-combustion capture techniques and plants. European best practice guidelines for assessment of CO2 capture technologies*, 2011, European Benchmarking Task Force.
17. de Visser, E., et al., *Dynamis CO2 quality recommendations.* International Journal of Greenhouse Gas Control, 2008. **2**(4): p. 478-484.

18. Lopes, F.V.S., et al., *Adsorption of H2, CO2, CH4, CO, N2 and H2O in Activated Carbon and Zeolite for Hydrogen Production.* Separation Science and Technology, 2009. **44**(5): p. 1045-1073.
19. Field, R.P. and R. Brasington, *Baseline Flowsheet Model for IGCC with Carbon Capture.* Industrial & Engineering Chemistry Research, 2011. **50**(19): p. 11306-11312.
20. NETL, *Cost and Performance Baseline for Fossil Energy Plants. Volume 1: Bitominous Coal and Natural Gas to Electricity*, 2013.
21. Casas, N., et al., *A parametric study of a PSA process for pre-combustion CO2 capture.* Separation and Purification Technology, 2013. **104**(0): p. 183-192.
22. Liu, Z., et al., *Multi-bed Vacuum Pressure Swing Adsorption for carbon dioxide capture from flue gas.* Separation and Purification Technology, 2011. **81**(3): p. 307-317.
23. Na, B.-K., et al., *Effect of Rinse and Recycle Methods on the Pressure Swing Adsorption Process To Recover CO2 from Power Plant Flue Gas Using Activated Carbon.* Industrial & Engineering Chemistry Research, 2002. **41**(22): p. 5498-5503.
24. Darde, A., et al., *Air separation and flue gas compression and purification units for oxy-coal combustion systems.* Energy Procedia, 2009. **1**(1): p. 527-534.
25. Pipitone, G. and O. Bolland, *Power generation with CO2 capture: Technology for CO2 purification.* International Journal of Greenhouse Gas Control, 2009. **3**(5): p. 528-534.
26. Posch, S. and M. Haider, *Optimization of CO2 compression and purification units (CO2CPU) for CCS power plants.* Fuel, 2012. **101**(0): p. 254-263.
27. Botero, C., et al., *The Phase Inversion-based Coal-CO2 Slurry (PHICCOS) feeding system: Technoeconomic assessment using coupled multiscale analysis.* International Journal of Greenhouse Gas Control, 2013. **18**(0): p. 150-164.
28. Siriwardane, R.V., et al., *Adsorption of CO2 on Molecular Sieves and Activated Carbon.* Energy & Fuels, 2001. **15**(2): p. 279-284.
29. Li, G., et al., *Capture of CO2 from high humidity flue gas by vacuum swing adsorption with zeolite 13X.* Adsorption, 2008. **14**(2-3): p. 415-422.
30. Ribeiro, A.M., et al., *Four beds pressure swing adsorption for hydrogen purification: Case of humid feed and activated carbon beds.* AIChE Journal, 2009. **55**(9): p. 2292-2302.
31. Arstad, B., et al., *Amine functionalised metal organic frameworks (MOFs) as adsorbents for carbon dioxide.* Adsorption, 2008. **14**(6): p. 755-762.
32. Casas, N., et al., *MOF and UiO-67/MCM-41 adsorbents for pre-combustion CO2 capture by PSA: Breakthrough experiments and process design.* Separation and Purification Technology, 2013. **112**(0): p. 34-48.
33. Hedin, N., L. Chen, and A. Laaksonen, *Sorbents for CO(2) capture from flue gas--aspects from materials and theoretical chemistry.* Nanoscale, 2010. **2**(10): p. 1819-41.
34. Lu, C., et al., *Comparative Study of CO2 Capture by Carbon Nanotubes, Activated Carbons, and Zeolites.* Energy & Fuels, 2008. **22**(5): p. 3050-3056.
35. Nitta, T., et al., *AN ADSORPTION ISOTHERM OF MULTI-SITE OCCUPANCY MODEL FOR HOMOGENEOUS SURFACE.* Journal of Chemical Engineering of Japan, 1984. **17**(1): p. 39-45.
36. Sumida, K., et al., *Carbon Dioxide Capture in Metal–Organic Frameworks.* Chemical Reviews, 2012. **112**(2): p. 724-781.